

Vibration and Buckling Characteristics of I-Shaped Steel Column Corroded on Boundary with Concrete

H. Kashiwa, H. Naito & M. Suzuki
University of Tohoku, Japan



SUMMARY:

Vibration characteristics of I-shaped steel columns corroded at their boundaries with concrete were investigated to obtain basic experimental data for a non-destructive inspection of steel-concrete composite joints. In electric corrosion tests of four I-shaped steel columns embedded in concrete, we examined the relationships between the corrosion ratio (amount of steel corrosion) and vibration characteristics (resonance frequency and damping coefficient). The resonance frequency of the concrete elements was decreased by steel corrosion in the concrete. The damping coefficients of the steel columns and concrete elements were increased by steel corrosion. In addition, a buckling finite element (FE) analysis of the steel columns corroded on the boundary with concrete was conducted, and we found that the buckling strength was proportionally decreased with the corrosion ratio. However, the buckling mode and buckling displacement changed depending on the details of the columns' sections, the height of the columns, and the corrosion ratio.

Keywords: steel-concrete composite structure, steel corrosion, vibration characteristic, buckling characteristic

1. INTRODUCTION

Steel-concrete composite structures are used for many bridges and buildings in Japan. In these composite joints, steel members are embedded into concrete slabs or concrete footings. Most of these structures were constructed 30 to 50 years ago, and there are many aging structures. Steel corrosion occurs at the boundary abutting the concrete. A non-destructive inspection method is necessary to evaluate the corrosion ratio of steel members embedded in concrete, as part of the maintenance of these aging composite structures. The evaluation of seismic performance (flexural stiffness, flexural strength and ductility, etc.) of I-shaped steel columns corroded in concrete is also very important in light of the frequent earthquakes in Japan. Decisions regarding the repair, reinforcement or replacement of corroded steel members and the rebuilding of bridges and aging structures with these steel columns are based on the steel components' damage level and seismic performance, and on the social use and importance of the structures. However, there are few studies describing non-destructive inspection methods or the seismic performance of I-shaped steel columns corroded on their boundaries with concrete.

In the present study, the vibration characteristics of I-shaped steel columns and concrete elements were investigated to obtain basic data for evaluating the corrosion ratios (i.e., the amount of steel corrosion) of steel-concrete composite joints. Four I-shaped steel columns embedded in concrete were corroded by direct-current electricity. We conducted forced vibration tests on the I-shaped steel columns and concrete elements. The relationship between corrosion ratio and these vibration characteristics was examined.

In addition, we conducted a buckling finite element (FE) analysis of I-shaped steel columns corroded on their boundaries with concrete to investigate the relationship between corrosion ratio and buckling characteristics such as buckling mode, buckling strength and buckling displacement.

2. VIBRATION CHARACTERISTICS

2.1. Outline of Experimental Tests

2.1.1. Test specimens

Details of the four I-shaped steel columns are given in Fig. 1. The four specimens were classified into two types. Specimens T-1 and T-2 simulated steel truss members that penetrated through concrete slabs; such steel truss members are used in many road bridges in Japan. Specimens C-1 and C-2 simulated I-shaped steel cantilever columns embedded in concrete footings. For all four specimens, the sectional size of the I-shaped steel columns was 100 mm x 100 mm x 6 mm x 8 mm (height of section, width of flange, thickness of web plate, thickness of flange plate). The corrosion lengths in concrete were 100 mm in Specimens T-1 and T-2, and those of Specimens C-1 and C-2 were 150 mm. Reinforcing steel bars (10-mm dia.) were arranged in the concrete components of all four specimens to restrain expanding cracks caused by steel corrosion. The material properties of the I-shaped steel and concrete are listed in Table 1.

2.1.2. Electric corrosion tests of I-shaped steel embedded in concrete

The I-shaped steel embedded in concrete was corroded by direct-current electricity. The electric corrosion test details are shown in Fig. 2. Wire sheets were embedded in the concrete facing the flange and web plate in order to corrode I-shaped steel uniformly. The target corrosion ratio was 20% for all specimens, and "corrosion ratio" was defined as the mass decrease ratio of steel in the corrosion region in concrete. All specimens were broken down after the electric corrosion tests, and the masses of the corroded I-shaped steel columns were measured.

2.1.3. Forced vibration tests of I-shaped steel columns

Resonance frequencies and damping coefficients of the I-shaped steel columns embedded in concrete were measured in forced vibration tests using a portable exciter. Excitation points and measurement response points are shown in Fig. 3. The harmonic vibration was given to each I-shaped steel column

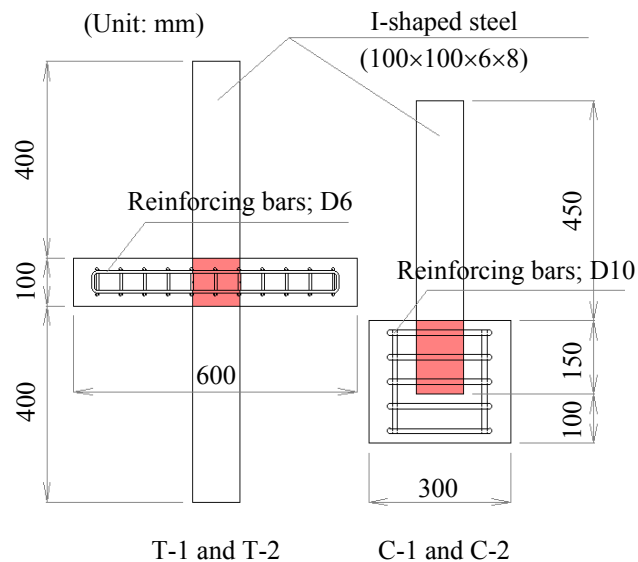


Figure 1. I-shaped steel and concrete specimens

Table 1. Material Properties Of The Steel And Concrete

| I-shaped steel | | | | Concrete | | | |
|-------------------------------------|---------------------------------------|----------------|------------------------------|---|--|--------------------------------------|------------------------------|
| Yield strength (N/mm ²) | Tensile strength (N/mm ²) | Elongation (%) | Density (kg/m ³) | Compressive strength (N/mm ²) | Dynamic elastic modulus (N/mm ²) | Young's modulus (N/mm ²) | Density (kg/m ³) |
| 346 | 452 | 32 | 7830 | 26.6 | 35100 | 28200 | 2390 |

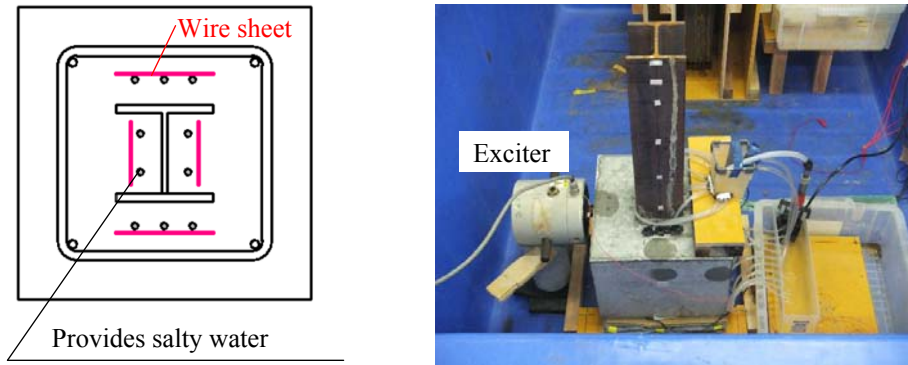


Figure 2. Electric corrosion test of I-shaped steel

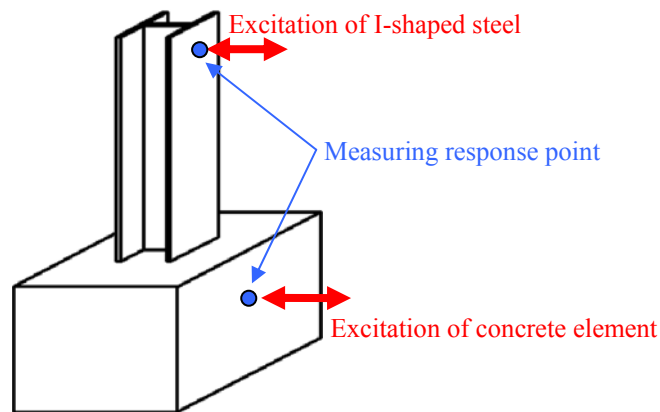


Figure 3. Excitation and measurement points

in strong axis by a portable exciter. The mass of the vibration table of the exciter was 0.13 kg, and the input acceleration was 2.0 m/s^2 . The sweep frequency was from 600 to 650 Hz, and the test time was 1 min. The response acceleration of the I-shaped steel column was measured by a piezoelectric-type acceleration pickup, and resonance curves were obtained. The acceleration pickup was pasted on the flange plate with double-faced tape. Details of the forced vibration testing method and the specifications of the measurement equipment are described in the author's previous paper (Naito and Ito et al. 2011; Watanabe et al. 2011).

2.1.4. Forced vibration tests of concrete elements

In the author's previous forced vibration tests of reinforced concrete beams and slab decks, the resonance frequencies were notably decreased by inner voids and cracks (Naito and Saiki et. al 2011). It was thought that the resonance frequency of the concrete element shown in Fig. 3 was also decreased by inner cracks caused by expansion of the steel corrosion and loss of the bond between the steel and the concrete boundary. As shown in Fig. 3, longitudinal harmonic vibration was applied to one side of the concrete element, and the response acceleration was measured to obtain the resonance curve. The excitation points and measuring response points are shown in Fig. 3. The input acceleration was 5.0 m/s^2 , and the sweep frequency was from 500 to 10,000 Hz. The test time was 4 min.

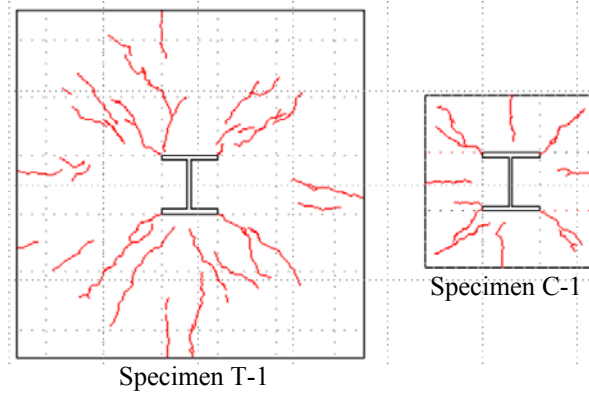
2.2. Experimental Results

2.2.1. Electric corrosion tests of I-shaped steel

The relationship between the corrosion ratio, R_{cor} , and visible damage states is described in Table 2. We found that the visible damage states of all four specimens did not differ significantly. Visible corrosion cracks on the concrete surfaces of Specimens T-1 (at $R_{cor} = 21.3\%$) and C-1 (at $R_{cor} = 12.4\%$) are shown as examples in Fig. 4. In Specimen T-1, rust on the steel at its concrete boundary appeared at $R_{cor} = 0.5\%$, and concrete cracks from the flange plate were also caused at $R_{cor} = 1.6\%$.

Table 2. Relationship Between The Corrosion Ratio And Visible Damage States

| | Appearance of steel rust | Concrete cracking at a right angle to flange plate | Concrete cracking in an oblique direction from edges of flange plate | Concrete cracking at a right angle to web plate |
|-----|--------------------------|--|--|---|
| T-1 | 0.5 % | 1.6 % | 2.7 % | 5.3 % |
| T-2 | 0.6 % | 1.2 % | 0.6 % | 2.5 % |
| C-1 | 0.3 % | 0.3 % | 0.6 % | 1.5 % |
| C-2 | 0.7 % | 0.7 % | 1.0 % | 1.3 % |

**Figure 4.** Corrosion cracks on the concrete surfaces

Concrete cracks in an oblique direction from the edges of the flange plates were caused at $R_{cor} = 2.7\%$, and concrete cracks from the web plate were also caused at $R_{cor} = 5.3\%$. In Specimen C-1, rust on the steel at the concrete boundary appeared at $R_{cor} = 0.3\%$, and concrete cracks from the flange plate were also caused at $R_{cor} = 0.3\%$. Concrete cracks in an oblique direction from the edges of the flange plates were caused at $R_{cor} = 0.6\%$, and concrete cracks from the web plate were caused at $R_{cor} = 1.5\%$.

After the electric corrosion tests, the four specimens were broken down and the steel columns were taken from their concrete elements. The masses of the corroded steel columns were measured. The corrosion ratios (R_{cor}) was defined as mass reduction in corrosion length. The R_{cor} values corresponded fairly well to the target values (20%) in Specimens T-1 and T-2, but those of Specimens C-1 and C-2 were approx 12%-13%, less than the target values.

2.2.2. Forced vibration tests of I-shaped steel columns

The resonance curves of the steel columns without corrosion damage were measured before the electric corrosion tests were performed. The resonance curves of Specimen C-1 is shown in Fig. 5. Here, the sweep frequencies ranged from 500 to 2,500 Hz in the forced vibration tests. The resonance frequencies of Specimens C-1 was 623 Hz. The resonance frequency in flexural vibration mode is theoretically obtained by the equation:

$$f_{lex} = \frac{1}{2\pi} \left(\frac{\lambda}{L} \right)^2 \sqrt{\frac{E_d I}{\rho A}} \quad (1)$$

where, f_{lex} is the resonance frequency, λ is 1.875, L is the length of the cantilever column, E_d is the dynamic elastic modulus of the steel, ρ is the density of the steel, I is the second moment of the area of the I-shaped steel, and A is the sectional area of the I-shaped steel. The theoretical resonance frequency, f_{lex} , is given as 609 Hz when $L = 450$ mm is assumed.

We examined the adequacy of the forced vibration tests by drawing Nyquist diagrams (the relationship between response acceleration and phase). Nyquist diagrams of Specimen C-1 without corrosion damage is shown in Fig. 5. The Nyquist diagram resulted in a round shape, confirming the accuracy of

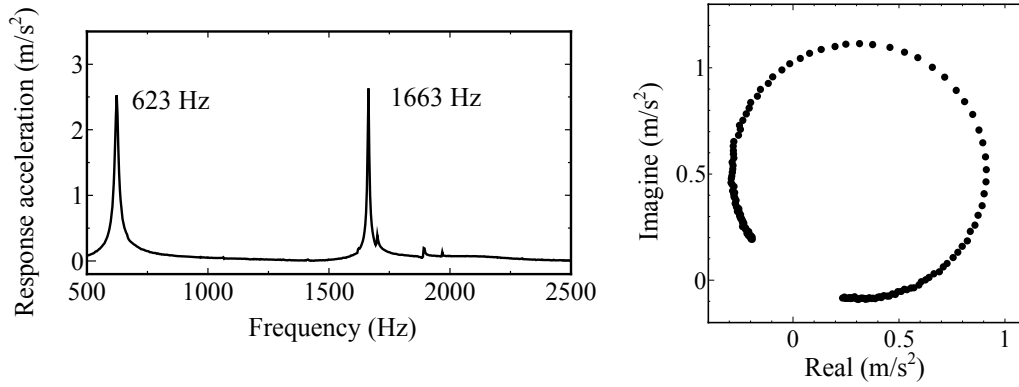


Figure 5. Resonance curve and Nyquist diagram of I-shaped steel column without corrosion (Specimen C-1)

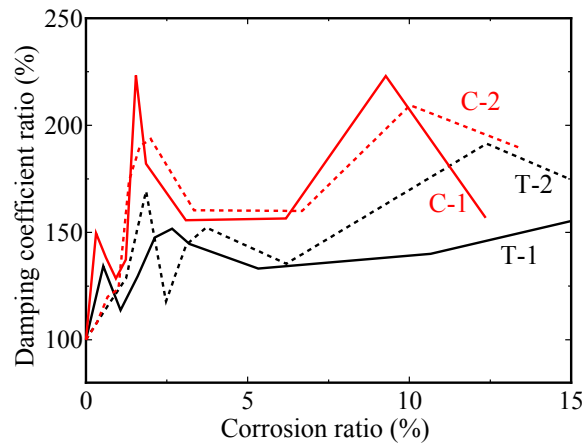


Figure 6. Relationship between the specimens' corrosion ratios and damping coefficients

the forced vibration tests. The damping coefficients of the four steel columns were obtained from the Nyquist diagrams by the half-power method. The relationship between the corrosion ratio R_{cor} values and the damping coefficients are given in Fig. 6, where the damping coefficients were normalized by the initial values without corrosion damage. For all four specimens, the damping coefficients were increased by steel corrosion. In particular, the damping coefficients were markedly increased when the corrosion ratio was less than 3%. This corrosion ratio ($R_{cor} = 3\%$) corresponded to concrete cracking caused by expansion of steel corrosion. In addition, the damping coefficients were moderately increased by steel corrosion when R_{cor} was greater than 3%.

In contrast, the resonance frequencies of the steel columns were not markedly changed. It was difficult to evaluate the corrosion ratios based on the resonance frequency changes.

2.2.3. Forced vibration tests of concrete elements

Resonance curves of the concrete elements without corrosion damage were measured before the electric corrosion tests were conducted. The resonance curve of the concrete element of Specimen C-1 is presented in Fig. 7. The sweep frequencies were from 1,000 to 10,000 Hz in these vibration tests. Some resonance frequencies are shown in the resonance curve. The resonance frequency in the longitudinal vibration mode f_{long} is theoretically obtained by the following equation:

$$f_{long} = \frac{1}{2t} \sqrt{\frac{E_d}{\rho}} \quad (2)$$

where f_{long} is the resonance frequency, t is the thickness of the concrete element in the excitation direction, E_d is the dynamic elastic modulus of the concrete, and ρ is the density of the concrete.

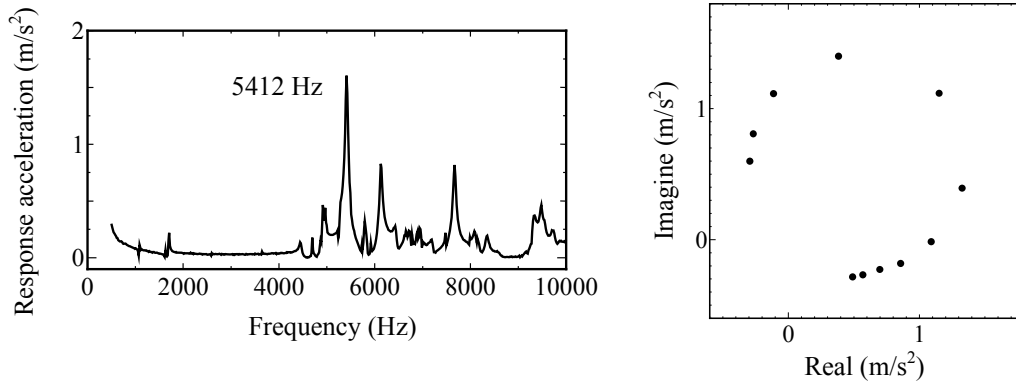


Figure 7. Resonance curve and Nyquist diagram of concrete element without damage (Specimen C-1)

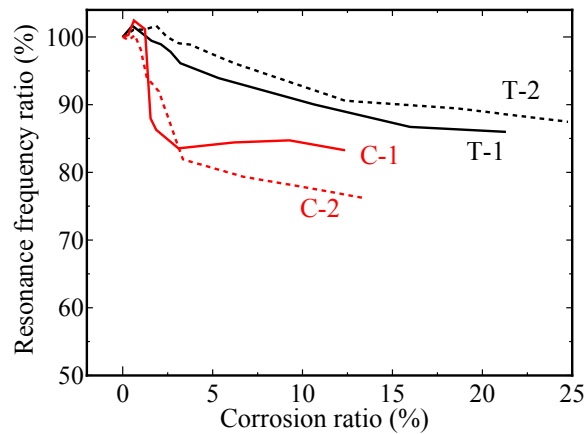


Figure 8. Relationship between corrosion ratios and resonance frequency ratios

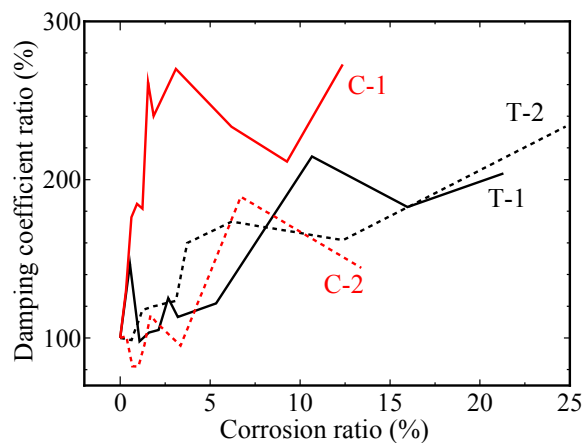


Figure 9. The relationship between corrosion ratios and damping coefficient ratios

The theoretical resonance frequency of Specimen C-1 was 6,387 Hz when the reinforced bars and the I-shaped steel were ignored. Referring to the theoretical value, the experimental resonance frequency was obtained as 5,412 Hz from the resonance curve, as shown in Fig. 7. The relationship between the corrosion ratio and resonance frequency values is plotted in Fig. 8, where resonance frequencies were normalized by initial values. The resonance frequencies of all specimens were decreased by steel corrosion. Concrete cracking and loss of steel-concrete bond were caused by steel corrosion in the concrete elements. We suspect that the damage to the concrete decreased the resonance frequencies of the concrete elements.

Nyquist diagrams were obtained by performing longitudinal vibration tests of the concrete elements.

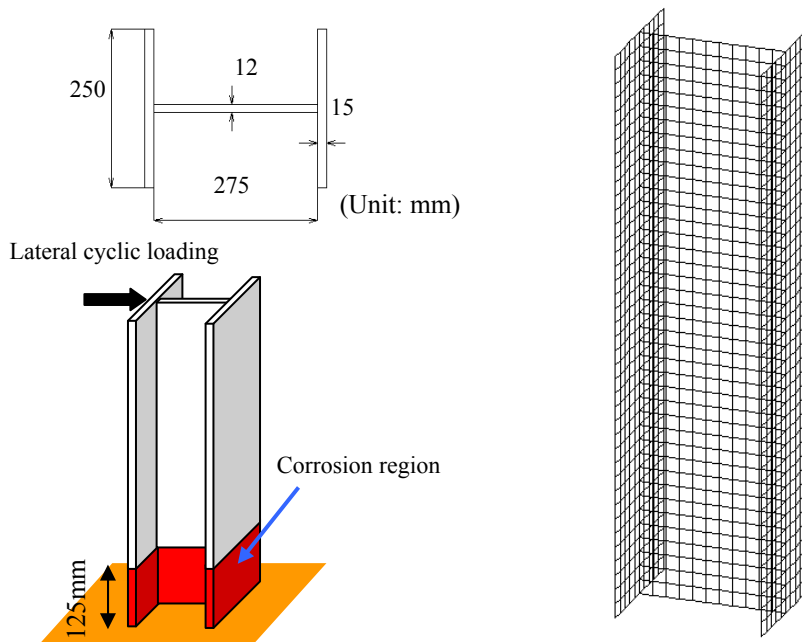


Figure 10. FE model of the I-shaped steel columns

Fig. 7 is the Nyquist diagram of Specimen C-1 without corrosion damage. The diagram shows a round shape, indicating the adequacy of the forced vibration test of concrete element. Fig. 9 shows the relationship between the corrosion ratios and damping coefficients, where the damping coefficients were normalized by initial values. The damping coefficients were notably increased by steel corrosion.

2.2.4. Conclusion of experimental tests

Our experiments' results indicate that the resonance frequencies of the concrete elements were notably decreased by steel corrosion, but the resonance frequencies of the I-shaped steel columns were not markedly changed. Moreover, the damping coefficients of the I-shaped steel columns and concrete elements were increased by steel corrosion. The changes in the damping coefficients were notable, but it was difficult to evaluate the initial values without corrosion damage because a damping coefficient was not obtained theoretically. The changes in the resonance frequency of the concrete elements were moderate. However, these initial values were obtained theoretically using the evaluation equation (Eqn. 2) and the material properties (density and dynamic elastic modulus) of the concrete.

From these experimental results, it was thought that the corrosion ratios of the steel columns embedded in concrete could be evaluated based on these vibration characteristics if more basic experimental data were obtained.

3. BUCKLING CHARACTERISTICS

3.1. Outline of Finite Element (FE) Model

We investigated the seismic performance of corroded I-shaped steel columns, and we examined the relationship between the corrosion ratio and buckling characteristics (buckling mode, buckling strength and buckling displacement) by using a three-dimensional finite element (FE) analysis. Details of the I-shaped steel columns and the FE model are given in Fig. 10. The sectional size of the I-shaped steel was 300 mm x 250 mm x 12 mm x 15 mm (height of section, width of flange, thickness of web, thickness of flange). The flange and web plates were modeled by 4-node shell elements. The bottom of the I-shaped steel column was fixed, and the top of the column was subjected to lateral reversed cyclic loading. The stress-strain relationship of the steel was obtained by a bilinear model. Young's modulus was 200,000 N/mm², Poisson's ratio was 0.3, the yield stress was 300 N/mm², and the hardening

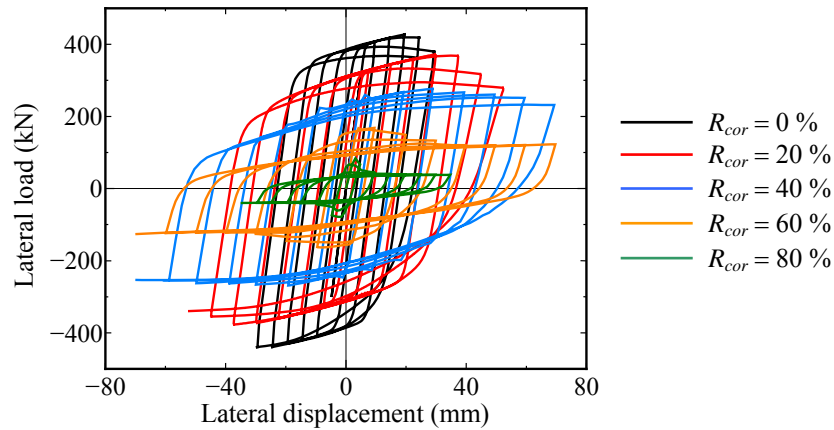


Figure 11. Lateral load and displacement relationship (column length: 1000 mm)

Table 3. Buckling Modes Of Corroded I-Shaped Steel

| | | Corrosion ratio (%) | | | | |
|--------------------|------|---------------------|-------|-------|-------|-------|
| | | 0 | 20 | 40 | 60 | 80 |
| Column length (mm) | 500 | Local | Local | Local | Local | Local |
| | 1000 | Torsion | Local | Local | Local | Local |
| | 2000 | Torsion | Local | Local | Local | Local |
| | 3000 | Torsion | Local | Local | Local | Local |
| | 4000 | Torsion | Local | Local | Local | Local |

Local: Local buckling of flange plate at the bottom of column Torsion: Global torsion buckling of column

coefficient was assumed to be 0.01 beyond that during yielding. The length of corrosion was 125 mm from the bottom of the column (see Fig. 10). Considering the steel corrosion, the thicknesses of the flange and web plates were reduced to 20%, 40%, 60% and 80%.

3.2. Calculating Results

The relationship between lateral load and displacement was calculated (see Fig. 11), and the buckling mode for each corrosion ratio is listed in Table 3. In the calculation without corrosion damage ($R_{cor} = 0\%$), the I-shaped steel columns buckled in the global torsion buckling mode when the lengths of the cantilever columns were greater than 1,000 mm. When the column length was 500 mm, the I-shaped steel column buckled as local buckling of the flange plate at the bottom of the column. With corrosion damage, however, all of the I-shaped steel columns buckled as local buckling of the flange plate in all combinations of corrosion ratio and column length.

The relationship between the corrosion ratio and buckling strength is illustrated in Fig. 12 (a), where buckling strengths were normalized by initial values without steel corrosion. Buckling strength corresponded to the maximum strength values obtained by the lateral load-displacement relationship, indicating that buckling strengths were linearly decreased by an increase in the corrosion ratio. The buckling strengths were equal to the yield strengths, because these I-shaped steel columns buckled in plasticity. The buckling strengths (equal to yield strengths) were proportional to the decrease in the sectional area caused by steel corrosion.

Fig. 12 (b) shows the relationship between the corrosion ratio and buckling displacement, where buckling displacement values were normalized by initial values without steel corrosion. As described above, the steel columns without steel corrosion buckled in the global torsion buckling mode when the lengths of the cantilever columns (L) were greater than 1000 mm. However, these buckling modes

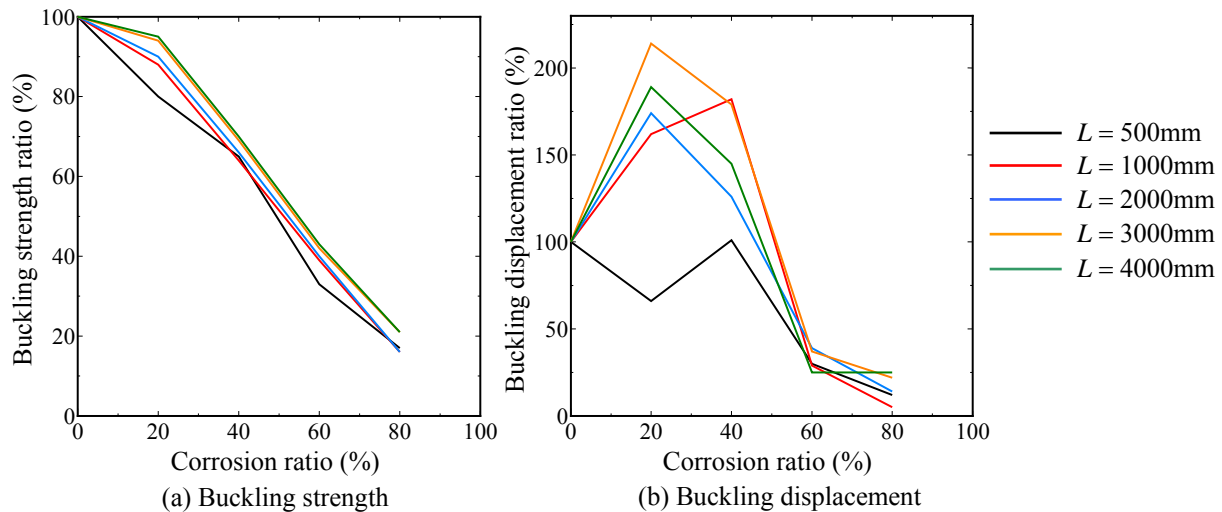


Figure 12. Relationship between corrosion ratios and buckling characteristics

changed to local buckling modes of flange plates when the steel corrosion was given in any case of corrosion ratio. In these columns (1000, 2000, 3000, and 4000 mm in length), buckling displacements were increased when the corrosion ratio was 20% or 40%. In contrast, the buckling mode was not changed by steel corrosion in the calculation results for the 500-mm-long column. The buckling displacement values were also not markedly changed when the corrosion ratio was 20% or 40%. Moreover, the buckling displacements of all of these I-shaped steel columns, at any column length (L), were notably decreased when the corrosion ratio was 60% or 80%.

4. CONCLUSIONS

We investigated the vibration and buckling characteristics of I-shaped steel corroded on the boundary with concrete, and we found that the resonance frequencies of the concrete elements were decreased by steel corrosion, whereas the resonance frequencies of the I-shaped steel columns were unchanged. In addition, the damping coefficients of both the I-shaped steel columns and the concrete elements were notably increased by steel corrosion.

In the calculation results, buckling strengths were linearly decreased by the increase in corrosion ratio. In some cases of corrosion ratio and height of the I-shaped steel columns, the buckling mode changed from the global torsion buckling mode to a local buckling mode of the flange plate at the bottom of the column when corrosion damage was included. In these corroded I-shaped steel columns, buckling displacements were increased when the corrosion ratio was 20% or 40%, and the buckling displacements of all of the I-shaped steel columns were notably decreased when the corrosion ratio was 60% or 80% in all values of column length.

Future studies will further evaluate the corrosion ratios and seismic performance of I-shaped steel columns embedded in concrete based on the vibration tests, when more basic experimental data are obtained.

REFERENCES

- Naito, H., Ito, T., Aoki, S. and Suzuki, M. (2011). Vibration characteristics of steel-concrete composite joints damaged with steel corrosion. *Journal of Structural Engineering* (Japan Society of Civil Engineers) **57A**, 1060-1073.
- Watanabe, T., Naito, H., Ohtake, Y. and Suzuki, M. (2011). A method for determining the location of cracks in concrete beam using anti-resonance frequency change. *Proceedings of ATEM'11* (International Conference on Advanced Technology in Experimental Mechanics 2011): OS11F024.

Naito, H., Saiki, Y., Suzuki, M., Iwaki, I., Koda, Y. and Kato, K. (2011). Non-destructive testing of concrete slab based on forced vibration test using portable shaker, *Journal of materials, concrete structures and pavements* (Japan Society of Civil Engineers) **67:4**, 522-534.